

Structure and Reactivity of Aquacarbonylruthenium(II) Complexes. An X-ray and Oxygen-17 NMR Study

Urs C. Meier, Rosario Scopelliti, Euro Solari, and André E. Merbach*

Institut de Chimie Minérale et Analytique, Université de Lausanne BCH,
CH-1015 Lausanne, Switzerland

Received March 1, 2000

The water exchange on $[\text{Ru}(\text{CO})(\text{H}_2\text{O}\text{-eq})_4(\text{H}_2\text{O}\text{-ax})](\text{tos})_2$ (**1**), $[\text{Ru}(\text{CO})_2(\text{H}_2\text{O}\text{-eq})_2(\text{H}_2\text{O}\text{-ax})_2](\text{tos})_2$ (**2**), and $[\text{Ru}(\text{CO})_3(\text{H}_2\text{O})_3](\text{ClO}_4)_2$ (**3**), the ^{17}O exchange between the bulk water and the carbonyl oxygens have been studied by ^{17}O NMR spectroscopy, and the X-ray crystallographic structures of **1** and **2** have been determined. The water exchange of equatorially and axially coordinated water molecules on **1** and **2** follow an I_d mechanism and are characterized by k_{eq}^{298} (s^{-1}), ΔH^\ddagger (kJ/mol), and ΔS^\ddagger ($\text{J}/(\text{mol K})$) of $(2.54 \pm 0.05) \times 10^{-6}$, 111.6 ± 0.4 , and 22.4 ± 1 (**1-eq**); $(3.54 \pm 0.02) \times 10^{-2}$ and 81 (**1-ax**); $(1.58 \pm 0.14) \times 10^{-7}$, 120.3 ± 2 , and 28.4 ± 4 (**2-eq**); and $(4.53 \pm 0.08) \times 10^{-4}$, 97.9 ± 1 , and 19.3 ± 3 (**2-ax**). The observed reactivities correlate with the strength of the Ru–OH₂ bonds, as expressed by their length obtained by X-ray studies: 2.079 (**1-eq**), 2.140 (**1-ax**), 2.073 (**2-eq**), and 2.110 (**2-ax**) Å. **3** is strongly acidic with a $\text{p}K_a$ of -0.14 at 262 K. Therefore, the acid-dependent water exchange can take place through **3** or $\text{Ru}(\text{CO})_3(\text{H}_2\text{O})_3\text{OH}^+$ with an estimated k_{eq}^{298} of $10^{-4}/10^{-3} \text{ s}^{-1}$ and k_{OH}^{262} of $0.053 \pm 0.006 \text{ s}^{-1}$. The ^{17}O exchange rate between the bulk water and the carbonyl oxygens increases from **1** to **2** to **3**. For **1** an upper limit of 10^{-8} s^{-1} was estimated. For **2**, no acid dependence of $k_{\text{Ru}^{\text{CO}}}$ between 0.1 and 1 m Htos was observed. At 312.6 K, in 0.1 and 1 m Htos, $k_{\text{Ru}^{\text{CO}}} = (1.18 \pm 0.03) \times 10^{-4}$. For the tricarbonyl complex, the exchange can proceed through **3** or $\text{Ru}(\text{CO})_3(\text{H}_2\text{O})_2\text{OH}^+$ with $k_{\text{Ru}^{\text{CO}}}$ and $k_{\text{RuOH}^{\text{CO}}}$ of, respectively, 0.003 ± 0.002 and $0.024 \pm 0.003 \text{ s}^{-1}$, with a ruthenacarbonylic acid intermediate.

Introduction

Interest in water-soluble organometallic compounds, particularly Ru(II), has increased in recent years, due to potential application in medicine and catalysis.^{1–3} As an example, hydrido, alkyl, acyl, aquo, and carbonyl complexes of Ru(II) are intermediates in the catalytic hydroxylation of ethene.⁴ To understand the catalytic cycles, a detailed knowledge of the reactivity and properties of all intermediates is required. Nowadays, ruthenium(II) aqua complexes can be conveniently synthesized from the $\text{Ru}(\text{H}_2\text{O})_6^{2+}$.⁵ Solvent exchange studies are fundamental to understand the reactivity of metal complexes, since they are a measure of the intrinsic reactivity of these complexes and it is possible to tune these properties by replacing one or several solvent molecules in the first coordination sphere of the complex by a variety of different ligands. Further, knowledge of the X-ray crystal structures makes it possible to correlate the reactivity of these complexes with structural parameters such as bond lengths and bond angles.⁶

In this paper, the water exchange on $\text{Ru}(\text{CO})(\text{H}_2\text{O})_5^{2+}$ (**1**) and $\text{cis-Ru}(\text{CO})_2(\text{H}_2\text{O})_4^{2+}$ (**2**) as a function of the temperature,

and on $\text{fac-Ru}(\text{CO})_3(\text{H}_2\text{O})_3^{2+}$ (**3**) as a function of the acid concentration, is studied by ^{17}O NMR spectroscopy. X-ray crystal structures of **1** and **2** are also determined, and a comparison of different ground-state properties with the observed reactivities is made.

Experimental Section

Chemicals and Solutions. $\text{Ru}(\text{H}_2\text{O})_6(\text{tos})_2$ ($\text{tos}^- = p$ -toluenesulfonate anion) and $[\text{RuCO}(\text{H}_2\text{O})_5](\text{tos})_2$ (**1**) were synthesized as described by Bernhard et al.⁵ and Laurenczy et al.⁷

cis-[Ru(CO)₂(H₂O)₄](tos)₂ (2**).** A 0.8 g (1.45 mmol) sample of $\text{Ru}(\text{H}_2\text{O})_6(\text{tos})_2$ and 0.298 g (1.56 mmol) of Htos (Fluka, 99%) were added to 5 g of D₂O (Amar, 99.95%) in an autoclave, and a pressure of 58 bar of CO was applied. This solution was stirred and heated to 348 K for one month. The solid complex was obtained quantitatively by evaporating the solvent under reduced pressure. IR (H₂O): 2023 cm⁻¹ (B₁), 2089 (A₁), relative intensities 3:2. ¹³C NMR: 194 ppm. ¹⁷O NMR: 368 (C=O, 2O), -48 (H₂O-ax, 2O), -133 (H₂O-eq, 2O) ppm.

fac-[Ru(CO)₃(H₂O)₃](ClO₄)₂ (3**).** **3** was synthesized in two steps. First, $\text{fac-RuCl}_2(\text{CO})_3(\text{THF})$ was obtained by recrystallizing $[\text{RuCl}_2(\text{CO})_3]_2$ (Strem Chemicals, 98%) in THF.⁸ In a second step 0.41 g (1.25 mmol) of $\text{fac-RuCl}_2(\text{CO})_3(\text{THF})$ was added to 1.8 g of H₂O, 1.51 g of 5 M HClO₄, and 0.566 g (2.51 mmol) of AgClO₄·H₂O (Fluka, 99%) at room temperature under vigorous stirring. After 4 min the solution was filtrated and the solvent evaporated under reduced pressure until the colorless $[\text{Ru}(\text{CO})_3(\text{H}_2\text{O})_3](\text{ClO}_4)_2$ complex precipitated. IR (H₂O): 2084 (E), 2170 (A₁) cm⁻¹, relative intensities 2:1. ¹³C NMR: 182 ppm. ¹⁷O NMR: 370 (C=O, 3O), -68 (H₂O, 3O) ppm. The IR frequencies and the ¹³C NMR chemical shift are in agreement with the data for the $[\text{Ru}(\text{CO})_3(\text{H}_2\text{O})_3](\text{BF}_4)_2$ complex published by Funaioli et al.⁵

* To whom correspondence should be addressed. Phone: +41 21 692 38 71. Fax: +41 21 692 38 75. E-mail: andre.merbach@icma.unil.ch.

- (1) Cauci, S.; Alessio, E.; Mestroni, G.; Quadrioglio, F. *Inorg. Chim. Acta* **1987**, *137*, 19–24.
- (2) Esposito, G.; Cauci, S.; Fogolari, F.; Alessio, E.; Scocchi, M.; Quadrioglio, F.; Viglino, P. *Biochemistry* **1992**, *31*, 7094–7103.
- (3) Fachinetti, G.; Funaioli, T.; Lecci, L.; Marchetti, F. *Inorg. Chem.* **1996**, *35*, 7217–7224.
- (4) Funaioli, T.; Cavazza, C.; Marchetti, F.; Fachinetti, G. *Inorg. Chem.* **1999**, *38*, 3361–3368.
- (5) Bernhard, P.; Bürgi, H.-B.; Hauser, J.; Lehmann, H.; Ludi, A. *Inorg. Chem.* **1982**, *21*, 3936–3941.
- (6) Bürgi, H.-B. In *Perspectives in Coordination Chemistry*; Williams, A. F., Floriani, C., Merbach, A. E., Eds.; Verlag Helv. Chim. Acta **1992**, 1–29.

(7) Laurenczy, G.; Helm, L.; Ludi, A.; Merbach, A. E. *Helv. Chim. Acta* **1991**, *74*, 1236–1238.

(8) Johnson, B. F. G.; Johnston, R. D.; Lewis, J. J. *Chem. Soc. A* **1969**, 792–797.

Table 1. Crystallographic Collection and Refinement Parameters for [Ru(CO)(H₂O)₅](tos)₂ (**1**) and *cis*-[Ru(CO)₂(H₂O)₄](tos)₂ (**2**)

	1	2
empirical formula	C ₁₅ H ₂₄ O ₁₂ RuS ₂	C ₁₆ H ₃₀ O ₁₆ Ru S ₂
fw	561.53	643.59
temp, K	143(2)	143(2)
wavelength	Mo K α	Mo K α
space group	C2/c	C2/c
<i>a</i> , Å	25.577(5)	30.795(2)
<i>b</i> , Å	6.8690(14)	6.9192(6)
<i>c</i> , Å	25.063(5)	12.2662(7)
β , deg	105.407(6)	106.54(3)
vol, Å ³	4221.0(15)	2519.7(3)
Z	8	4
density (calcd), Mg/m ³	1.767	1.697
abs coeff, mm ⁻¹	1.001	0.861
final <i>R</i> indices [<i>I</i> > 2 σ (<i>I</i>)]	R1 ^a = 0.0591, wR2 ^b = 0.1776	R1 ^a = 0.0513, wR2 ^b = 0.1343
<i>R</i> indices (all data)	R1 ^a = 0.0662, wR2 ^b = 0.1878	R1 ^a = 0.0520, wR2 ^b = 0.1348

$${}^a R1 = \sum ||F_o| - |F_c|| / \sum |F_o|. \quad {}^b wR2 = \{ \sum [w(F_o^2 - F_c^2)] / \sum [w(F_o^2)] \}^{1/2}.$$

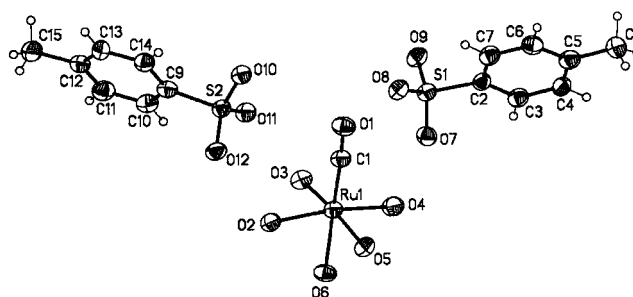
IR Measurements. IR spectra in aqueous solution of all complexes were recorded on a Matteson FT-IR spectrophotometer using CaF₂ windows and a 12 μ m path length.

X-ray Experimental Section. Crystals of [RuCO(H₂O)₅](tos)₂ and [Ru(CO)₂(H₂O)₄](tos)₂, suitable for X-ray diffraction, were obtained through slow evaporation of aqueous solutions containing an excess of Htos and mounted in glass capillaries. Crystal data and structure refinement details are listed in Table 1. Data were collected for **2** on a Kuma κ CCD and reduced with CrysAlis Red release 1.6.2 (Kuma Diffraction Instruments GmbH, PSE-EPSL module 3.4, CH-1015 Lausanne, Switzerland, 1999), whereas for **1** data collection was performed on a mar345 imaging plate detector system and reduced with marHKL release 1.9.1.⁹ No absorption correction was applied to all data sets. Structure solution for both compounds was performed by ab initio direct methods.¹⁰ All structures were refined by full-matrix least-squares on *F*² with all non-H atoms anisotropically defined. H atoms were placed in calculated positions using the "riding model" (except the ones belonging to water molecules in **2**) with *U*_{iso} = *aU*_{eq}(*X*) (where *a* is 1.5 for methyl hydrogen atoms and 1.2 for others, while *X* is the parent atom). Space group determination, structure solution and refinement, molecular graphics, and geometrical calculation on all structures have been carried out using the SHELXTL software package, release 5.1 (Bruker AXS, Inc., Madison, WI, 53719, 1997). Final atomic coordinates, thermal and geometrical parameters, and hydrogen coordinates are given in the Supporting Information.

NMR Measurements. The ¹⁷O and ¹³C NMR spectra were recorded on Bruker ARX-400 and DPX-400 NMR spectrometers at 54.25 and 100.63 MHz, respectively. The ¹⁷O NMR spectra were referenced to the bulk water signal ($\delta = 0$ ppm) and the ¹³C NMR spectra to TMS and measured with respect to the methyl carbon of tos ($\delta = 22.9$ ppm).

¹⁷O NMR Spectra. The parameters were chosen to obtain quantitative spectra. A 90° pulse of 15 μ s, an acquisition time of 20–50 ms, and a sweep width of 55.5 kHz were used and from 512 to 20k scans accumulated per spectrum. The temperature was measured by a substitution technique.¹¹ Solutions of 5–10% isotopically enriched ¹⁷-OH₂ were used.

Kinetic Studies. The water oxygen and carbonyl oxygen exchange on **1**, **2**, and **3** was monitored by following the evolution of the ¹⁷O enrichment as a function of time. Since the water exchange rates of axially and equatorially coordinated water molecules differ by more than 2 orders of magnitude in the case of the mono- and biscarbonyl complexes, the two reactions could be treated independently. The rate law for the isotopic exchange is given by eq 1, where *x* and *x*_∞ are the

**Figure 1.** ORTEP view of [Ru(CO)(H₂O)₅](tos)₂ (**1**).**Table 2.** Selected Bond Length (Å) and Angles (deg) for [Ru(CO)(H₂O)₅](tos)₂

Ru(1)–C(1)	1.813(5)	Ru(1)–O(3)	2.084(3)
Ru(1)–O(2)	2.073(3)	Ru(1)–O(6)	2.140(3)
Ru(1)–O(4)	2.076(4)	C(1)–O(1)	1.159(6)
Ru(1)–O(5)	2.083(3)		
C(1)–Ru(1)–O(2)	94.10(18)	O(4)–Ru(1)–O(3)	89.34(15)
C(1)–Ru(1)–O(4)	96.24(19)	O(5)–Ru(1)–O(3)	172.81(13)
O(2)–Ru(1)–O(4)	169.45(15)	C(1)–Ru(1)–O(6)	175.23(18)
C(1)–Ru(1)–O(5)	92.3(2)	O(2)–Ru(1)–O(6)	84.74(14)
O(2)–Ru(1)–O(5)	92.50(14)	O(4)–Ru(1)–O(6)	85.12(15)
O(4)–Ru(1)–O(5)	89.17(16)	O(5)–Ru(1)–O(6)	83.15(16)
C(1)–Ru(1)–O(3)	94.87(19)	O(3)–Ru(1)–O(6)	89.72(14)
O(2)–Ru(1)–O(3)	87.71(14)	O(1)–C(1)–Ru(1)	176.5(4)

mole fractions of labeled oxygen in coordinated water or CO molecules in a particular site at times *t* and *t*_∞ and *k* is the pseudo-first-order exchange rate constant.

$$-dx/dt = k(x - x_{\infty})/(1 - x_{\infty}) \quad (1)$$

Experimentally, the mole fractions are given by eq 2, where [H₂¹⁷O]_f and [¹⁷O]_c are, respectively, the concentrations of the labeled free and coordinated oxygen, and *I*_f and *I*_c the integrals of the corresponding NMR signals.

$$x = [{}^{17}\text{O}]_c / ([{}^{17}\text{O}]_c + [\text{H}_2{}^{17}\text{O}]_f) = I_c / (I_c + I_f) \quad (2)$$

For a two-site exchange, integration of eq 1 gives eq 3.

$$x = x_{\infty} + (x_0 - x_{\infty}) \exp(-kt/(1 - x_{\infty})) \quad (3)$$

Results and Discussion

[RuCO(H₂O)₅](tos)₂. The crystal structure shows the expected octahedral coordination geometry around the ruthenium(II) (Figure 1 and Table 2). The first coordination sphere is made of one carbon monoxide ligand and two different sets of bound water, one axially and four equatorially coordinated H₂O molecules which are, respectively, in *cis* and *trans* positions relative to the carbon monoxide ligand. Ru–O bond lengths for the axial and the four equatorial water molecules are, respectively, 2.140(3) and 2.079(3) Å (average). A rather short Ru–CO distance of 1.813(5) Å is present and in agreement with a long CO bond of 1.159(6) Å. The ¹³C and ¹⁷O solution NMR spectra with the observed signals of axially and equatorially coordinated H₂O in a 1:4 ratio at, respectively, –29 and –155 ppm in the ¹⁷O NMR spectra and the resonance at 206 ppm in the ¹³C NMR spectra⁷ are in full agreement with the octahedral coordination geometry observed in the solid state (Table 3).

The *cis* water exchange on **1** could be studied between 298 and 342 K by the isotopic enrichment method. The rate constants as a function of the temperature are shown in Figure S1 and Table S1 in the Supporting Information. The enthalpy and entropy of activation are, respectively, 111.6 ± 0.4 kJ/mol and

(9) Otwinowski, Z.; Minor, W. In *Macromolecular Crystallography*; Carter, C. W., Jr., Sweet, R. M., Eds.; Academic Press: New York, 1997; pp 307–326.

(10) Sheldrick, G. M. *Acta Crystallogr.* **1990**, *A46*, 467.

(11) Amman, C.; Meier, P.; Merbach, A. E. *J. Magn. Reson.* **1982**, *46*, 319–321.

Table 3. ^{13}C and ^{17}O NMR Chemical Shifts (ppm) of the Mono, Bis, and Tris Ruthenium Carbonyl Aqua Complexes

	H_2O		$\text{C}\equiv\text{O}$	
	^{17}O -eq	^{17}O -ax	^{17}O	^{13}C
$[\text{Ru}(\text{H}_2\text{O})_6](\text{tos})_2^a$		-192		
$[\text{RuCO}(\text{H}_2\text{O}\text{-eq})_4(\text{H}_2\text{O}\text{-ax})](\text{tos})_2$	-155	-29	358	206
<i>cis</i> - $[\text{Ru}(\text{CO})_2(\text{H}_2\text{O}\text{-eq})_2(\text{H}_2\text{O}\text{-ax})_2](\text{tos})_2$	-133	-48	368	194
<i>fac</i> - $[\text{Ru}(\text{CO})_3(\text{H}_2\text{O})_3](\text{ClO}_4)_2^b$		-68	370	182

^a Reference 19. ^b 2 m HClO_4 .

22 ± 1 J/(mol K). Exchange of the axially coordinated water molecule is characterized by a ΔH^\ddagger of 81 kJ/mol (Table 4). The small temperature range accessible for studying this reaction, 274–298 K, excluded the meaningful determination of ΔS^\ddagger .

***cis*- $[\text{Ru}(\text{CO})_2(\text{H}_2\text{O})_4](\text{tos})_2$.** The molecular structure of **2** shows the expected octahedral coordination geometry around the ruthenium(II) (Figure 2 and Table 5). The two carbonyl groups are in *cis* positions with respect to each other. Water molecules bound in the equatorial positions (*cis* with respect to both CO groups) have a significantly shorter Ru–O bond length (2.073(3) Å) than the water molecules in the axial positions (2.110(4) Å), which are *trans* to one CO and *cis* to the other CO group, displaying a structural *trans* influence. The Ru–O bond length of H_2O bound in equatorial sites belongs to the shortest known bond distances in Ru(II) complexes and may be regarded as the lower limit for Ru–O bond distances.¹² A Ru–CO distance of 1.877(5) Å corresponds to the average observed for terminal Ru–CO bond lengths,¹² and the CO bond length of 1.138(6) Å is slightly larger than for gaseous CO (1.128 Å).

The ^{17}O NMR spectrum of **2** shows three signals at 368, -48, and -133 ppm which are, respectively, assigned to the carbonyl oxygen and the axially and equatorially coordinated water molecules. In the ^{13}C NMR spectra, the bis complex is characterized by a single resonance at 194 ppm (Table 3). These data are in complete agreement with an octahedral ruthenium(II) complex having a first coordination sphere made of two carbonyl groups in positions *cis* to each other and two sets of two water molecules, as determined by the X-ray crystallographic structure (Figure 2). On the basis of analogy with complex **1**, the observed water exchange kinetics (see below), and the Ru–O bond lengths, the water signal at higher frequency is assigned to the axial water and the signal at -133 ppm to the equatorial ones. A *trans* CO complex is not formed, since it is strongly disfavored by the π acceptor properties of the CO ligand.

Rate constants for the water exchange in the equatorial and axial positions were, respectively, determined between 312 and 354 K and between 279 and 314 K using a fast injection device.¹³ The rate constants as a function of the temperature are shown in Figure S1. Enthalpies and entropies of activation for the water exchange in the axial and equatorial positions are, respectively, 98 ± 1 and 120 ± 2 kJ/mol and 19 ± 3 and 28 ± 4 J/(mol K) (Table 4).

It is tempting to ascribe the observed lower reactivity of **2** compared to **1** and the different reactivities of the axially and equatorially bound water molecules to changes in the ground-state Ru–OH₂ bond lengths as determined by the X-ray

crystallographic structures. A correlation between the observed reactivities and ground-state properties requires the knowledge of the water exchange mechanism.^{14,15} Recently, it has been shown that the mono complex formation of $\text{Ru}(\text{H}_2\text{O})_6^{2+}$ with a variety of ligands having different nucleophilicities and the equatorial and axial water exchange on $\text{Ru}(\text{C}_2\text{H}_4)(\text{H}_2\text{O})_5^{2+}$ follows an I_d or D mechanism.^{16–18} Given the similar and positive entropies of activation for the water exchange in the equatorial and axial positions of the mono- and biscarbonyl complexes (see Table 4), it is reasonable to assign an I_d mechanism to the water exchange reaction for the two sites on both complexes. The structural changes undergone by an octahedral Ru(II) complex on the way to the transition state of a dissociatively activated ligand substitution reaction include the lengthening of the bond between the Ru(II) and the leaving H_2O molecule. If we assume that the energy required to reach the transition state is higher for the rupture of a short, energetically more stable bond than for the rupture of a longer, less stable bond between the same type of atoms, the observed trend in the exchange rates should be mirrored by the bond length differences in the ground states. Since the entropies of activation are very similar (between 19 and 28 J/(mol K); see Table 4), the activation process is likely similar in all these cases, and the enthalpy of activation simply corresponds to the energy required to elongate the Ru–O bond from the equilibrium distance to the distance at which the rupture of this bond occurs. This distance can be estimated using a harmonic oscillator model¹⁴ and the known activation enthalpies and bond lengths obtained from the crystal structures. The relation between these quantities is given by eq 4. k is the Ru–O force constant, R_{eq}

$$\Delta H^\ddagger = k(R^\ddagger - R_{\text{eq}})^2 \quad (4)$$

the equilibrium bond length and R^\ddagger the transition state bond length. Assuming that R^\ddagger and k are the same for the equatorial and axial Ru–O bonds, R^\ddagger can be calculated. R^\ddagger is estimated to be 2.48 Å (2.49 Å for **1** and 2.46 Å for **2**). An Ru–O bond elongation of ~ 0.4 Å is therefore required to reach the transition state.

Substituting a H_2O ligand on **1** by a CO decreases the reactivity of the H_2O bound in the axial and equatorial sites from 3.54×10^{-2} to 4.53×10^{-4} s⁻¹ and from 2.54×10^{-6} to 1.58×10^{-7} s⁻¹, respectively, at 298.15 K (Table 4). The larger, 78-fold decrease in reactivity for the axial sites as compared to the 16-fold decrease of the equatorial one is mirrored by the extent of the Ru–OH₂ bond shortening of, respectively, 0.030 and 0.006 Å from 2.140 to 2.110 Å and from 2.079 to 2.073 Å. The shortest Ru–O bond length of 2.073 Å in **2** is in agreement with the low reactivity of the equatorially coordinated water, which is the slowest measured water exchange rate on Ru(II) complexes.^{16,19–21}

In **1** and **2** the reactivities of the axial and equatorial water molecules differ considerably. The kinetic *trans* effect may be expressed by the ratio of $k_{\text{ax}}/k_{\text{eq}}$. This effect is more pronounced for the mono than the bis complex, despite the lower water exchange rates in **2**. For example, at 298.15 K the ratio is 13 900

(12) Orpen, A. G.; Allen, F. H.; Kennard, O.; Watson, D. G.; Taylor, R. J. *Chem. Soc., Dalton Trans.* **1989**, S1–S83.

(13) Bernhard, P.; Helm, L.; Ludi, A.; Merbach, A. E. *J. Am. Chem. Soc.* **1985**, *107*, 312–317.

(14) Elder, R. C.; Heeg, M. J.; Payne, M. D.; Trkula, M.; Deutsch, E. *Inorg. Chem.* **1978**, *17*, 431–440.

(15) Schwarzenbach, G.; Bürgi, H.-B.; Jensen, W. P.; Lawrance, G. A.; Monsted, L.; Sargeson, A. M. *Inorg. Chem.* **1983**, *22*, 4029–4038.

(16) Aebischer, N.; Sidorenkova, H.; Ravera, M.; Laurency, G.; Osella, D.; Weber, J.; Merbach, A. E. *Inorg. Chem.* **1997**, *36*, 6009–6020.

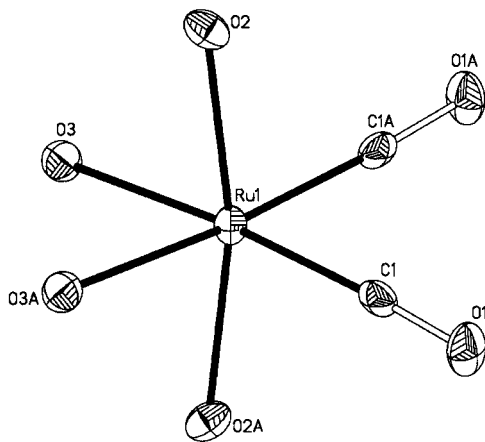
(17) Aebischer, N.; Churlaud, R.; Dolci, L.; Frey, U.; Merbach, A. E. *Inorg. Chem.* **1998**, *37*, 5915–5924.

(18) Aebischer, N.; Laurency, G.; Ludi, A.; Merbach, A. E. *Inorg. Chem.* **1993**, *32*, 2810–2814.

Table 4. Activation Parameters for the Water Exchange in the Equatorial and Axial Positions on $[\text{Ru}(\text{CO})(\text{H}_2\text{O})_5](\text{tos})_2$ and $\text{cis}-[\text{Ru}(\text{CO})_2(\text{H}_2\text{O})_4](\text{tos})_2$

complex	$k_{298.15}$ (s^{-1})	ΔH^\ddagger [kJ/mol] ^a	ΔS^\ddagger [J/(mol K)] ^a
$[\text{RuCO}(\text{H}_2\text{O}\text{-eq})_4(\text{H}_2\text{O}\text{-ax})](\text{tos})_2$	$(2.54 \pm 0.05) \times 10^{-6}$	111.6 ± 0.4	22.4 ± 1
$[\text{RuCO}(\text{H}_2\text{O}\text{-eq})_4(\text{H}_2\text{O}\text{-ax})](\text{tos})_2$	$(3.54 \pm 0.02) \times 10^{-2}$	81	<i>b</i>
$\text{cis}-[\text{Ru}(\text{CO})_2(\text{H}_2\text{O}\text{-eq})_2(\text{H}_2\text{O}\text{-ax})_2](\text{tos})_2$	$(1.58 \pm 0.14) \times 10^{-7}$	120.3 ± 2	28.4 ± 4
$\text{cis}-[\text{Ru}(\text{CO})_2(\text{H}_2\text{O}\text{-eq})_2(\text{H}_2\text{O}\text{-ax})_2](\text{tos})_2$	$(4.53 \pm 0.08) \times 10^{-4}$	97.9 ± 1	19.3 ± 3

^a Errors are given as 1 standard deviation. ^b Temperature range too small to be meaningful (274–297 K).

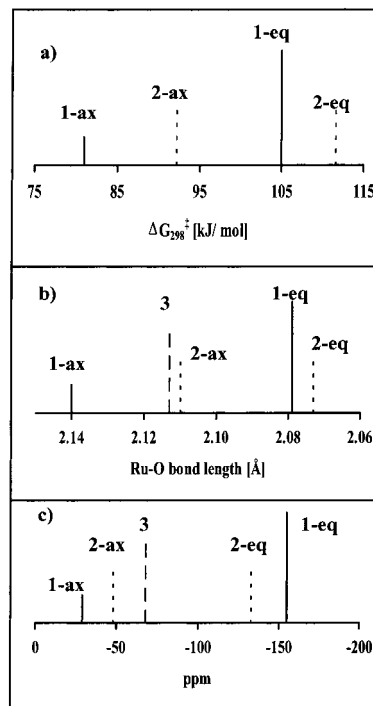
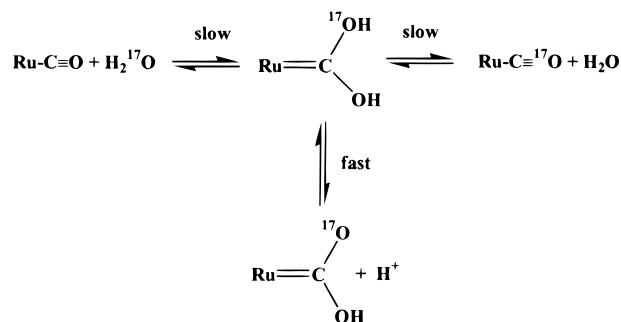
**Figure 2.** ORTEP view of $\text{cis}-[\text{Ru}(\text{CO})_2(\text{H}_2\text{O})_4](\text{tos})_2$ (**1**). Hydrogen atoms have been omitted for clarity. The letter A indicates the following symmetry transformation $-x, y, -z + 1/2$.**Table 5.** Selected Bond Lengths (Å) and Angles (deg) for $\text{cis}-[\text{Ru}(\text{CO})_2(\text{H}_2\text{O})_4](\text{tos})_2$

Ru(1)–C(1)	1.877(5)	Ru(1)–O(3)	2.110(4)
Ru(1)–O(2)	2.073(3)	C(1)–O(1)	1.138(6)
C(1)–Ru(1)–C(1A)	87.4(3)	C(1)–Ru(1)–O(3A)	92.85(18)
C(1)–Ru(1)–O(2)	95.90(17)	O(2)–Ru(1)–O(3)	88.59(14)
C(1)–Ru(1)–O(2A)	92.54(17)	O(2)–Ru(1)–O(3A)	82.82(14)
O(2)–Ru(1)–O(2A)	168.3(2)	O(3)–Ru(1)–O(3A)	85.3(2)
C(1)–Ru(1)–O(3)	175.29(17)	O(1)–C(1)–Ru(1)	176.5(4)

for **1** and 2900 for **2**. Structural trans influences of, respectively, 0.061 and 0.037 Å for **1** and **2** in the reactant ground state are in agreement with the observed water exchange kinetics. These structural and kinetic data clearly demonstrate that the CO ligand exerts predominantly a cis effect and influences the water in a trans position to a much lesser extent. The greater structural differences between equatorial and axial water molecules in **1** compared to **2** are also reflected by the chemical shift difference between the two types of water molecules of, respectively, 136 and 85 ppm for **1** and **2** (Figure 3).

fac- $[\text{Ru}(\text{CO})_3(\text{H}_2\text{O})_3](\text{ClO}_4)_2$. The ^{17}O NMR spectra of **3** in 5 m HClO_4 displays signals at 370 and -68 ppm corresponding, respectively, to the carbon monoxide and coordinated water oxygen and the ^{13}C NMR spectra one signal at 182 ppm in agreement with the presence of the facial isomer only. The equal ^{17}O integrals of the CO and H_2O signals further confirm that, in strongly acidic solution, **3** is exclusively present as a monomer, as observed in the solid state.⁴ No condensation products are observed under these conditions.

The composition of a solution made of **3** is pH dependent. Lowering the $[\text{HClO}_4]$ below 2 m results in the appearance of a new peak in the CO as well as a second one in the H_2O region at, respectively, 353 and -46 ppm. The two new signals increase further with decreasing acid concentration. In 0.44 m HClO_4 , the ratio between **3** and the newly formed species is 7:1. The formation of the new species is fully reversible, and on addition of HClO_4 , the new signals disappear again, proving the presence

**Figure 3.** Graphical representation of (a) ΔG_{298}^\ddagger for the water exchange, (b) Ru–O bond lengths, and (c) ^{17}O NMR chemical shifts of $[\text{Ru}(\text{CO})(\text{H}_2\text{O}\text{-eq})_4(\text{H}_2\text{O}\text{-ax})](\text{tos})_2$ (**1**, —), $\text{cis}-[\text{Ru}(\text{CO})_2(\text{H}_2\text{O}\text{-eq})_2(\text{H}_2\text{O}\text{-ax})_2](\text{tos})_2$ (**2**, ···) and $\text{fac}-[\text{Ru}(\text{CO})_3(\text{H}_2\text{O})_3](\text{ClO}_4)_2$ (**3**, ---).**Scheme 1**

of a pH-controlled equilibrium. The same behavior has been observed by Funaioli et al.⁴ by ^{13}C NMR spectroscopy on ^{13}C -enriched **3** and was attributed to the formation of a ruthenacetic acid (Scheme 1). Further, at 275 K, no decomposition of **3** in 0.44 m HClO_4 was observed over a period of 10 days. The integrals of the bound CO and H_2O of **3** at, respectively, 370 and -68 ppm are equal at all $[\text{HClO}_4]$ values used, confirming the monomeric nature of **3** under these conditions.

3 is of limited stability, as it decomposed within minutes at temperatures above 350 K in 1 m HClO_4 . This decomposition is accompanied by a color change from colorless to yellow. The same is observed in 0.1 m HClO_4 , but at 320 K. On the basis of a signal at -14 ppm in the ^1H NMR spectra and the appearance of CO_2 in the IR spectra, the formation of a

monohydride biscarbonyl complex, *fac*-[RuH(CO)₂(H₂O)₃]⁺ (**4**), was proposed by Funaioli et al.⁴ In agreement with that assignment, we observed in the coupled ¹³C NMR spectra a doublet at 196 ppm with ²J_{C-H} = 10.5 Hz and in the ¹⁷O NMR spectra three signals at 349, 78, and -51 ppm in a 2:1:2 ratio which are respectively assigned to the carbon monoxide and the H₂O ligand *trans* and the two H₂O ligands *cis* relative to the hydride ligand.

The remarkable stability of **4** in strongly acidic solution is due to the π acceptor properties of the CO groups, which considerably reduce the electron density at the Ru(II) center and consequently the proton affinity of the hydride ligand. This is in agreement with the observed high acidity of dicationic dihydrogen complexes with π acid ligands.^{22,23} For example, [M(H₂)CO(Ph₂P(CH₂)₃PPh₂)₂]²⁺, with M = Ru²⁺ and Os²⁺, have estimated pK_a values of, respectively, -6 and -5.7.²⁴ The reduced electron density at the metal center is best illustrated by the CO stretching frequencies of a series of homoleptic d⁶ low-spin metal carbonyl cations of Re⁺, Os²⁺, and Ir³⁺ whose frequencies increase from 2084 to 2190 to 2254 cm⁻¹.²⁵ Within the same group only slight variations are observed. As an example, the CO stretching frequencies vary from 2204 to 2199 to 2190 cm⁻¹ for Fe(CO)₆²⁺, Ru(CO)₆²⁺, and Os(CO)₆²⁺.^{25,26} The same behavior is observed for the d⁶ low-spin M(CO)₃(H₂O)₃ complexes of the group 7 (Mn⁺, Re⁺) and 8 (Ru²⁺) cations, but their stretching frequencies are smaller. Within group 7 the stretching frequencies change from 1944 and 2051 cm⁻¹ for *fac*-Mn(CO)₃(H₂O)₃⁺ to 1916 and 2036 cm⁻¹ for *fac*-Re(CO)₃(H₂O)₃⁺,²⁷ whereas the group 8 *fac*-Ru(CO)₃(H₂O)₃²⁺ stretching frequencies of 2084 and 2170 cm⁻¹ are more than 100 cm⁻¹ higher.

The water exchange rate constants on **3** at 262.25 K as a function of the HClO₄ concentration are shown in Figure 4a. They increase with decreasing acid concentration, which is an indication of an exchange pathway involving a hydrolyzed species. The nonlinearity of *k*_{obs} as a function of 1/[H⁺] is indicative of a proton dissociation of **3** (eqs 5a and 5b) in the [H⁺] range of this study.



$$K_a = [\text{Ru}(\text{CO})_3(\text{H}_2\text{O})_2(\text{OH})^+][\text{H}^+]/[\text{Ru}(\text{CO})_3(\text{H}_2\text{O})_3^{2+}] \quad (5b)$$

The ¹⁷O transverse relaxation rate of coordinated water, 1/*T*_{2,obs}, as a function of 1/[H⁺] (Figure 4b) displays the same curvature as *k*_{obs}, which is reminiscent of a very fast acid–base equilibrium (eqs 5a and 5b), leading to the observation of a

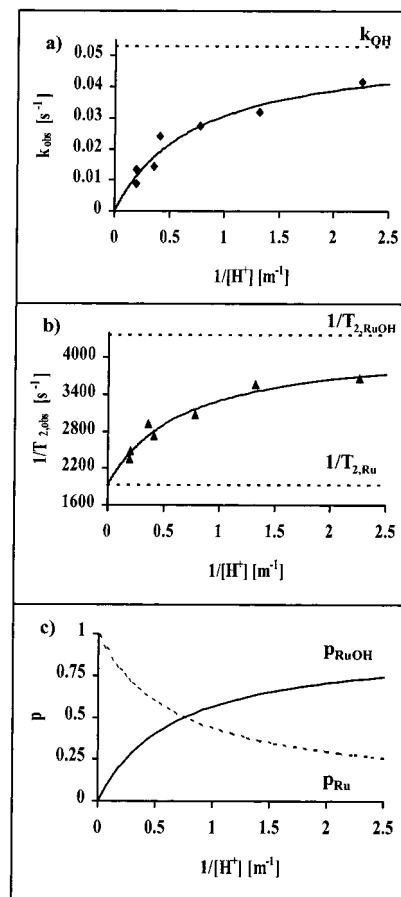


Figure 4. (a) Water exchange rate constants (◆) and (b) coordinated ¹⁷O transverse relaxation rates (%) and calculated mole fractions of Ru(CO)₃(H₂O)₃²⁺ and Ru(CO)₃(H₂O)₂(OH)⁺ as a function of 1/[H⁺] at 262.3 K. The solid lines correspond to the best fit obtained using eqs 5–8.

weighted average signal line width. This is also in agreement with a decreasing line width with increasing temperature, as expected for quadrupolar relaxation. It is important to note that the observed curvature in Figure 4a,b cannot be due to changes in viscosity, since the ¹⁷O NMR line width of the perchlorate and the carbonyl signals are invariant with respect to the HClO₄ concentration.

The *k*_{obs} and 1/*T*_{2,obs} are therefore directly related to eqs 6 and 7, with the populations of Ru(CO)₃(H₂O)₃²⁺, *p*_{Ru}, and Ru(CO)₃(H₂O)₂(OH)⁺, *p*_{RuOH}, given by eq 8.

$$k_{\text{obs}} = p_{\text{Ru}}k_{\text{ex}} + p_{\text{RuOH}}k_{\text{OH}} \quad (6)$$

$$1/T_{2,\text{obs}} = p_{\text{Ru}}(1/T_{2,\text{Ru}}) + p_{\text{RuOH}}(1/T_{2,\text{RuOH}}) \quad (7)$$

$$p_{\text{Ru}} = [\text{H}^+]/([\text{H}^+] + K_a) \quad \text{and} \quad p_{\text{RuOH}} = K_a/([\text{H}^+] + K_a) \quad (8)$$

Fitting eq 6 to eq 8, with five adjustable parameters, simultaneously to the experimental data gives a *k*_{ex} value (-0.002 ± 0.007 s⁻¹) equal to zero within experimental error. The water exchange rate constant *k*_{ex} of **3** is too small to be determined experimentally in the presence of even small amounts of the much more reactive monohydroxo species. However, an estimation of *k*_{ex} can be made from a comparison of ¹⁷O NMR chemical shifts and Ru–O bond length with the other carbonyl aqua congeners. Parts c and b of Figure 3 show that the ¹⁷O NMR shift (-68 ppm) and the Ru–O bond length (2.113 Å) of **3** are close to those of the axial water molecules

(19) Rapaport, I.; Helm, L.; Bernhard, P.; Ludi, A.; Merbach, A. E. *Inorg. Chem.* **1988**, *27*, 873–879.

(20) Luginbühl, W.; Zbinden, P.; Pittet, P.-A.; Armbruster, T.; Bürgi, H.-B.; Merbach, A. E.; Ludi, A. *Inorg. Chem.* **1991**, *30*, 2350–2355.

(21) Stebler-Röthlisberger, M.; Hummel, W.; Pittet, P.-A.; Bürgi, H.-B.; Ludi, A.; Merbach, A. E. *Inorg. Chem.* **1988**, *27*, 1358–1363.

(22) Landau, S. E.; Morris, R. H.; Lough, A. J. *Inorg. Chem.* **1999**, *38*, 6060–6068.

(23) Schlaf, M.; Lough, A. J.; Morris, R. H. *Organometallics* **1993**, *12*, 3808–3809.

(24) Rocchini, E.; Mezzetti, A.; Rügger, H.; Burckhardt, U.; Gramlich, V.; Del Zotto, A.; Martinuzzi, P.; Rigo, P. *Inorg. Chem.* **1997**, *36*, 711–720.

(25) Willner, H.; Aubke, F. *Angew. Chem., Int. Ed.* **1997**, *36*, 2402–2425.

(26) Bernhardt, E.; Bley, B.; Wartchow, R.; Willner, H.; Bill, E.; Kuhn, P.; Sham, I. H. T.; Bodenbinder, M.; Bröckler, R.; Aubke, F. *J. Am. Chem. Soc.* **1999**, *121*, 7188–7200.

(27) Kölle, U., and Ulrich, S. Personal communication.

(28) Alberto, R.; Egli, A.; Abram, U.; Hegetschweiler, K.; Gramlich, V.; Schubiger, P. A. *J. Chem. Soc., Dalton Trans.* **1994**, 2815–2820.

of **2** (−48 ppm and 2.110 Å). From this comparison, the order of magnitude of k_{ex} can be estimated between 10^{-4} and 10^{-3} s^{−1} at 298 K, and between 10^{-6} and 10^{-5} s^{−1} at the temperature of the experiment (262 K).

Therefore, k_{ex} could be neglected, and the fitting procedure was repeated with only four adjustable parameters, leading to $k_{\text{OH}} = 0.053 \pm 0.006$ s^{−1}, $K_{\text{a}} = 1.37 \pm 0.36$ M, $1/T_{2,\text{Ru}} = 1930 \pm 170$ s^{−1}, and $1/T_{2,\text{RuOH}} = 4370 \pm 220$ s^{−1}.

For the group 7 tricarbonyl aqua cations the water exchange rate constants decrease as expected for transition-metal cations, going from the first to the second and to the third row d⁶ cation. For example, the water exchange rate constants for Mn(CO)₃-(H₂O)₃⁺,²⁷ Tc(CO)₃(H₂O)₃⁺,²⁹ and Re(CO)₃(H₂O)₃⁺³⁰ are, respectively, 0.43, 5.38×10^{-2} , and 3.18×10^{-4} s^{−1} at 277 K. Surprisingly, the decrease of the water exchange rate between Mn⁺ and Tc⁺ is smaller than between Tc⁺ and Re⁺. At 277 K an order of magnitude of 10^{-5} to 10^{-4} s^{−1} is estimated for Ru(CO)₃(H₂O)₃²⁺, 3 orders of magnitude smaller than observed for Tc(CO)₃(H₂O)₃⁺. A decrease of the reactivity with increasing compactness of the metal center has also been observed for the water exchange on homoleptic d⁶ low-spin aqua complexes of Ru²⁺ (73 pm) and Rh³⁺ (66.5 pm). At 298 K the water exchange rate constant decreases from 0.018 s^{−1} for Ru²⁺ (I_d-D)¹⁹ to 2.2×10^{-9} s^{−1} for Rh³⁺ (I_a).³¹

It is interesting to compare the influence of the tricarbonyl moiety with the influence exerted by π-arene ligands such as benzene or Cp* (Cp* = η⁵-pentamethylcyclopentadienyl anion) on the solvent exchange rates. The benzene and Cp* ligands are known to increase the reactivity of coordinated solvent considerably compared to the homoleptic solvent complexes of d⁶ cations, with the increase being more pronounced for Cp*.^{21,32} As an example, $k_{\text{ex}}^{298/\text{s}^{-1}}$ ($\Delta H^\ddagger/\text{kJ mol}^{-1}$) values of, respectively, 8.9×10^{-11} (140.3), 4.07×10^{-5} (102.5), and 5.6 (86.5) were measured for Ru(CH₃CN)₆²⁺, (C₆H₆)Ru(CH₃CN)₃²⁺, and Cp*Ru(CH₃CN)₃⁺.³³ In the case of the aqua complexes, the reactivity increases from 0.018 s^{−1} for Ru(H₂O)₆²⁺ to 11.5 s^{−1} for (C₆H₆)Ru(H₂O)₃²⁺ at 298.15 K, but decreases to $10^{-4}/10^{-3}$ s^{−1} in the case of a tricarbonyl ligand set, despite the fact that the Ru–O bond lengths of 2.112, 2.117, and 2.113 Å are very similar. The bond lengths do not correlate with the observed reactivity and therefore are assigned to the bonding properties of the spectator groups.

At 262 K, the water exchange on Ru(CO)₃(H₂O)₂(OH)⁺, 0.053 s^{−1}, is 10³ to 10⁴ times faster than on Ru(CO)₃(H₂O)₃²⁺. This increase in reactivity of the hydroxo species is in the range observed for a variety of M³⁺ aqua ions, M = Ga, Ti, Fe, Cr, Ru, Rh, and Ir, for which accelerations between 75 (Cr³⁺) and 19 100 (Rh³⁺) at 298K were measured.³⁴ However, there is no apparent correlation between the acceleration of the water exchange on the hydroxide and the pK_a of the aqua complex.

The pK_a of −0.14 for **3** is much lower than expected for a M(OH₂)₆²⁺ (pK_a = 8–10) cation. Again the strong acidity of **3** is due to the π acceptor properties of the CO ligand, which reduces the electron density at the metal center. As a consequence of the reduced electron density at the metal center, the

O–H bonds are more polarized than in the case of Ru(H₂O)₆²⁺, and therefore, the acidity of the coordinated water is increased. Ru(CO)₃(H₂O)₃²⁺ behaves more like an M³⁺ than an M²⁺ transition-metal cation. This is similar to Re^I(CO)₃(H₂O)₃⁺ (pK_a = 7.5),³⁵ which behaves more like an M²⁺ than an M⁺ (pK_a = 13–15).

The increase of the transverse relaxation rate of Ru(CO)₃-(H₂O)₂OH⁺ (4370 s^{−1}) compared to **3** (1930 s^{−1}) is due to the reduced symmetry of the electron distribution around the oxygen atom in the case of the coordinated hydroxide compared to coordinated water, which increases the electric field gradient and consequently the line width.

It has been shown that the CO ligand exerts predominantly a cis effect on **1**; i.e., the reactivity of the H₂O bound in cis (equatorial) positions is massively reduced compared to that of the Ru(H₂O)₆²⁺, whereas that of the trans (axial) H₂O is only slightly increased.¹⁶ Comparing the reactivities of the water molecules with the number of CO ligands in cis and trans positions to it clearly shows that the cis effect of the CO ligand levels off after the first CO in a cis position. As an example, the water exchange rate constants of the axial H₂O in **2**, which has one CO in a cis position and one in a trans position, corresponds to the estimated constant for the H₂O exchange on **3**, which has two CO ligands in cis position and one in a trans position. For the equatorial water molecules in **1** and **2**, which have, respectively, one and two CO ligands in cis positions, only a 16-fold difference in the water exchange rates is measured. In the case of the axial H₂O of **1**, which has one CO trans to it, and **2**, which has one CO trans and one cis to it, a 78-fold difference is observed. Qualitatively, the ground-state properties, i.e., Ru–O bond lengths and chemical shifts, display the same behavior (Figure 3). The observed Ru–O bond lengths and the ¹⁷O NMR chemical shifts of H₂O in the equatorial positions of **1** (2.079 Å, −155 ppm) and **2** (2.073 Å, −133 ppm) and the axial positions of **2** (2.110 Å, −48 ppm) and in **3** (2.113 Å, −68 ppm) behave similarly (Figure 3b,c). These results clearly show that the influence of several CO ligands is not simply additive.

Fast ¹⁷O Enrichment of the Carbonyl Ligands. An exchange between ¹⁷O-enriched water and the carbon monoxide was observed, indicating a water gas shift related chemistry shown in Scheme 1. For **1** only an upper limit for the pseudo-first-order rate constant of 10^{-8} s^{−1} at 353 K could be estimated, due to the slow decomposition of the complex. For **2** and **3** it was also possible to study the ¹⁷O exchange on the carbon monoxide by ¹⁷O NMR spectroscopy. For **2**, no significant dependence of k_{CO} on [H⁺] was observed between 0.1 and 1 m Htos. As an example, in 0.1 and 1 m Htos a k_{CO} of, respectively, $(4.44 \pm 0.01) \times 10^{-5}$ and $(3.96 \pm 0.07) \times 10^{-5}$ s^{−1} at 303.1 K and $(1.18 \pm 0.01) \times 10^{-4}$ and $(1.18 \pm 0.03) \times 10^{-4}$ s^{−1} at 312.6 K were measured. The absence of a [H⁺] dependence is also observed for the axial water exchange on **2** (Figure S1).

In the case of **3**, k_{CO} is dependent on [H⁺] (Table 6). The k_{CO} decreases with increasing [H⁺]. The exchange rate constant increases with decreasing acid concentration (Table 6), as already observed for the water exchange (see above). To analyze the acid dependence, exchanges on Ru(CO)₃(H₂O)₃²⁺ and Ru(CO)₃(H₂O)₂OH⁺ were considered (eq 9).

$$k_{\text{CO}} = p_{\text{Ru}}k_{\text{Ru}}^{\text{CO}} + p_{\text{RuOH}}k_{\text{RuOH}}^{\text{CO}} \quad (9)$$

(29) Aebischer, N.; Schibli, R.; Alberto, R.; Merbach, A. E. *Angew. Chem., Int. Ed.* **2000**, *39*, 254–256.

(30) Hedinger, R., and Frey, U. Personal communication.

(31) Laurenczy, G.; Rapaport, I.; Zbinden, D.; Merbach, A. E. *Magn. Reson. Chem.* **1991**, *29*, S45–51.

(32) Dadci, L.; Elias, H.; Frey, U.; Hörnig, A.; Kölle, U.; Merbach, A. E.; Paulus, H.; Schneider, J. S. *Inorg. Chem.* **1995**, *34*, 306–315.

(33) Lincoln, S. F.; Merbach, A. E. *Adv. Inorg. Chem.* **1995**, *42*, 1–88.

(34) Cusanelli, A.; Frey, U.; Richens, D. T.; Merbach, A. E. *J. Am. Chem. Soc.* **1996**, *118*, 5265–5271.

(35) Egli, A.; Hegetschweiler, K.; Alberto, R.; Abram, U.; Schibli, R.; Hedinger, R.; Gramlich, V.; Kissner, R.; Schubiger, P. A. *Organometallics* **1997**, *16*, 1833–1840.

Table 6. Pseudo-First-Order Rate Constants, k_{CO} , for the ^{17}O Exchange between the Bulk and the Carbonyl Oxygen on $[\text{Ru}(\text{CO})_3(\text{H}_2\text{O})_3](\text{ClO}_4)_2$ at Various $[\text{HClO}_4]$ Values

[acid] (m)	T [K]	k_{CO} for 3 (s^{-1})	[acid] (m)	T [K]	k_{CO} for 3 (s^{-1})
0.44	262.3	$(1.64 \pm 0.08) \times 10^{-2}$	2.76	262.3	$(8.31 \pm 0.05) \times 10^{-3}$
0.76	262.3	$(1.57 \pm 0.1) \times 10^{-2}$	4.97	262.3	$(6.14 \pm 0.07) \times 10^{-3}$
1.28	262.3	$(1.48 \pm 0.01) \times 10^{-2}$	5.06	262.3	$(5.78 \pm 0.03) \times 10^{-3}$
2.41	262.3	$(1.38 \pm 0.08) \times 10^{-2}$			

Fitting eqs 8 and 9 to k_{CO} with $k_{\text{Ru}}^{\text{CO}}$ and $k_{\text{RuOH}}^{\text{CO}}$ as adjustable parameters and $K_{\text{a}} = 1.37 \text{ M}$, gives $k_{\text{RuOH}}^{\text{CO}} = 0.024 \pm 0.003 \text{ s}^{-1}$ and $k_{\text{Ru}}^{\text{CO}} = 0.003 \pm 0.002 \text{ s}^{-1}$ at 262.3 K (fit shown in the Supporting Information). The ^{17}O enrichment proceeds mainly through the hydrolyzed species.

The relative rates of ^{17}O exchange between the carbon monoxide of **1**, **2**, and **3** and the bulk water can be understood on the basis of the electrophilic character of the carbon atom in the different complexes, since the exchange is believed to occur by a nucleophilic attack at a carbon atom by H_2O ,^{36,37} forming a ruthenacaroxylic acid intermediate (see Scheme 1).⁵ The Ru–C σ -bond is formed from an unshared pair of electrons located on the carbon atom; an increase in this donation will result in a decrease in electron density on the carbon. Back-bonding in the CO π^* orbital, mainly located on the carbon,^{38,39} results in an increase of electron density at the carbon and weakens the C \equiv O bond strength. Due to the increased competition between the carbonyl ligands in **3** and **2** compared to **1** for the electron density available for back-bonding, the electrophilic character of the carbon atom increases from **1** to

2 to **3**, making it more susceptible to nucleophilic attack by H_2O . The increased electrophilic character of the carbon atom is also in agreement with the Ru–C and the C \equiv O bond length and the measured stretching frequencies for these complexes. The crystal structures for **1**, **2**, and **3**⁴ show a large increase of the Ru–CO bond length from 1.813 to 1.877 to 1.923 Å with an associated small decrease in the C \equiv O distance from 1.158 to 1.138 to 1.115 Å, with the carbonyl stretching frequencies increasing from 1970 to 2023/2089 to 2086/2170 cm^{-1} .

A faster exchange on $\text{Ru}(\text{CO})_3(\text{H}_2\text{O})_2(\text{OH})^+$ than on **3** is rather surprising, since the electrophilic character of the carbon atom in $\text{Ru}(\text{CO})_3(\text{H}_2\text{O})_2(\text{OH})^+$ is reduced compared to that in **3**. However, this behavior can be related to the fact that the exchange rate constant for the ^{17}O exchange between the bulk and the carbonyl oxygen ($0.024 \pm 0.003 \text{ s}^{-1}$) is roughly half the rate constant for the water exchange on $\text{Ru}(\text{CO})_3(\text{H}_2\text{O})_2(\text{OH})^+$ ($0.053 \pm 0.006 \text{ s}^{-1}$) at 262.3 K. A possible explanation of this behavior is an intramolecular nucleophilic attack by a coordinated H_2O , which is much more labile in $\text{Ru}(\text{CO})_3(\text{H}_2\text{O})_2(\text{OH})^+$ than in **3**. Within this picture the slower ^{17}O carbonyl exchange on **3** should occur by a nucleophilic attack by bulk water.

Acknowledgment. We thank the Swiss National Science Foundation for financial support and Dr. Nicolas Aebischer for his assistance and for useful discussions.

Supporting Information Available: Initial reactant concentrations and rate constants as a function of temperature for $\text{Ru}(\text{CO})_x(\text{H}_2\text{O})_{6-x}^{2+}$, rate constants as a function of $[\text{HClO}_4]$ for *fac*- $\text{Ru}(\text{CO})_3(\text{H}_2\text{O})_3^{2+}$, and tables of crystal data, atomic parameters, bond lengths and angles, anisotropic displacement parameters, and hydrogen coordinates for $\text{Ru}[(\text{CO})(\text{H}_2\text{O})_5](\text{tos})_2$ and *cis*- $\text{Ru}[(\text{CO})_2(\text{H}_2\text{O})_4](\text{tos})_2$. This material is available free of charge via the Internet at <http://pubs.acs.org>.

(36) Kump, R. L.; Todd, L. J. *Inorg. Chem.* **1981**, *20*, 3715–3717.(37) Darensbourg, D. J.; Darensbourg, M. Y. *Inorg. Chem.* **1970**, *9*, 1691–1694.(38) Block, T. F.; Fenske, R. F.; Casey, C. P. *J. Am. Chem. Soc.* **1976**, *98*, 441–443.(39) Lichtenberger, D. L.; Fenske, R. F. *Inorg. Chem.* **1976**, *15*, 2015–2022.